数理解析研究所講究録
第539巻 1984年 136-156

Fine Structure of Interaction of Shock Wave with Boundary Layer

大林 茂

Shigeru Obayashi

Department of Aeronautics, The University of Tokyo.

Abstract

The approximate LU factored method is developed to efficiently compute the compressible Navier-Stokes equations. The resulting method is employed to solve the two-dimensional interaction problems of shock wave with boundary layer on a flat plate and an airfoil. The flow fields are precisely simulated by mesh refinement.

§1. Introduction

The compressible Navier-Stokes equations have been used in computational fluid dynamics in order to solve interaction problems of shock wave with boundary layer. It is difficult to precisely simulate such flow fields because of the large amount of computational time and computer storage. The development of efficient methods for the compressible Navier-Stokes equations is desired.

Various factorization or splitting of the implicit procedure

of finite-difference methods in delta-form can be applied to improve convergence rates for steady-state problems. Some attempts for the Euler equations have been made by employing the local eigensystem/1/, such as the diagonal form/2/ and the flux vector splitting/3/. The use of the local eigensystem implies an implicit upwind difference algorithm where only a lower or upper bidiagonal matrix appears and the inversion is easier than that of tridiagonal matrix. Such algorithm has an advantage over stability and efficiency.

In this paper, the approximate LU factored method is developed. The matrices in implicit procedure are decomposed to the product of the lower and upper bidiagonal ones by the LU factorization derived from the ideas of the flux vector splitting and the implicit MacCormack method/4/. The resulting method is of $O(\Delta t, \Delta x^2)$ and reduces the CPU time and the temporary storage.

The two-dimensional interaction problems of shock wave with boundary layer are solved by employing the present method. One is the problem on a flat plate. The mesh is refined to precisely simulate a flow field. The other is that around an NACA0012 airfoil. The effects on the pattern of variations in Reynolds number and Mach number are investigated.

§2. Algorithm Development

A. Basic Algorithm

The governing equations of compressible viscous fluid are the compressible Navier-Stokes equations. They are written in

the conservation-law form. For brevity, a one-dimensional equation of conservation laws is at first considered in order to construct the new scheme and to analize its stability. The resulting scheme is then extended to the compressible Navier-Stokes equations in the following section.

A model equation is written as,

$$u_t+f_x=0, \tag{1}$$

where u is the density, f is its flux, and the subscripts t and x denote partial differentiations. This system can be rewritten as,

$$u_t+a(u)u_x=0. \tag{2}$$

where $a=\partial f/\partial u$, if $f=f(u)$. The standard implicit finite-differece method in delta form can be employed to seek steady-state solutions:

$$(1+\theta hDa)\Delta u_i^n=-hD(f_i^n), \tag{3}$$

where $u_i^n=u(i\Delta x,n\Delta t)$, $D(f_i)=f_{i+1/2}-f_{i-1/2}$, $Da\Delta u_i^n=D(a\Delta u_i^n)$, $h=\Delta t/\Delta x$ and θ is a number between 0 and 1.

First, let f be a function of u. This case implies the Euler equations. The flux f on half mesh-points are evaluated as,

$$f_{i\pm 1/2}=(f_i+f_{i\pm 1})/2. \tag{4}$$

Therefore the differece operator $D(f_i)$ results in the second-order central differece for first derivatives; $D(f_i)=(f_{i+1}-f_{i-1})/2$. The linearized coefficients $a_{i\pm 1/2}$ can be chosen/5/ as

$$a_{i\pm 1/2}=c_{i\pm 1/2}=\left(\frac{\partial f}{\partial u}\right)^{n}_{i\pm 1/2}. \tag{5}$$

The central finite-difference can be replaced by the sum of the upwind differece, using the flux vector splitting technique/3/:

$$D(c\Delta u)=D_-(c^+\Delta u)+D_+(c^-\Delta u), \tag{6}$$

where $c^+=(c+|c|)/2$, $c^-=(c-|c|)/2$, $D_-(c^+\Delta u_i)=c^+\Delta u_i-c^+\Delta u_{i-1}$ and $D_+(c^-\Delta u_i)=c^-\Delta u_{i+1}-c^-\Delta u_i$.

The modified implicit procedure of Eq.(3) is rewritten as,

$$(1+\theta h(D_-c^++D_+c^-))\Delta u_i^n=-hD(f_i^n). \tag{7}$$

The usual Neumann's stability analysis for a constant coefficient results in the condition of θ such that $\theta\geq 1/2$. This scheme is second-order accurate when $\theta=1/2$. The first-order scheme, when $\theta=1$, is adequate to calculate a steady-state solution and thus used here. The left-hand-side of Eq.(7) can be replaced by the LU factored form suggested in Ref.3, because $h^2=O(\Delta t^2)$.

$$(1+hD_-c^+)(1+hD_+c^-)\Delta u_i^n=-hD(f_i^n). \tag{8}$$

For a linearized analysis, this factorization introduces no error since $c^+c^-=0$. The above operators, $(1+hD_-c^+)$ and $(1+hD_+c^-)$, lead to the lower and upper triangular matrices, respectively. This form requires no inversion of tridiagonal matrices.

Next, let f be a linear function of u_x, that is, $f=-\mu u_x$ where $\mu>0$ is the viscosity. This case implies the diffusion equations. The values of the flux f on half mesh points are calculated by the following equations,

$$f_{i\pm 1/2}=f(D_\pm(u_i)/\Delta x). \tag{9}$$

In this case, $a_{i\pm 1/2}$ describe the differece operators/6/, $-\mu D_\pm(*)/\Delta x$, because,

$$\Delta f_{i\pm 1/2}^n=-\mu D_\pm(\Delta u_i^n)/\Delta x+O(\Delta t^2). \tag{10}$$

The implicit scheme Eq.(3) is written as,

$$(1+\theta h(\mu D_-/\Delta x-\mu D_+/\Delta x))\Delta u_i^n=-hD(f_i^n), \tag{11}$$

where θ must satisfy $\theta\geq(2h\mu-\Delta x)/4h\mu$ for the stability and $\theta=1$ is sufficient for a steady-state solution. Eq.(11) can be written in the LU factored form like Eq.(8),

$$(1+hkD_-)(1-hkD_+)\Delta u_i^n=-hD(f_i^n). \tag{12}$$

where $k=\mu/\Delta x$.

Finally, let f be the sum of functions of u and u_x, that is, $f(u,u_x)=f_1(u)+f_2(u_x)$. This case implies the Navier-Stokes equations. The evaluations on half mesh-points are described as Eqs.(4) and (9) for f_1 and f_2, respectively. The change of the flux f in time is estimated as follows,

$$\Delta f^n=c\Delta u^n+\mu D_{\pm}(\Delta u^n)/\Delta x+O(\Delta t^2). \tag{13}$$

Corresponding to Eqs.(7) and (11), Eq.(3) can be rewritten as,

$$(1+h(D_-(|c^+|+k)-D_+(|c^-|+k)))\Delta u_i^n=-hD(f_i^n). \tag{14}$$

The resulting LU factored form is written as,

$$\begin{gathered}(1+hD_-\hat{a}^+)(1-hD_+\hat{a}^-)\Delta u_i^n=-hD(f_i^n),\\ \hat{a}^{\pm}=|c^{\pm}|+k.\end{gathered} \tag{15}$$

This implicit procedure is of $O(\Delta t)$, but it does not affect the accuracy of a steady-state solution if it exists uniquely. This scheme is of $O(\Delta x^2)$ at a steady state.

The present method is extended to the two-dimensional problem by modifying the standard implicit ADI factored scheme, not by applying the LU factored form proposed by Jameson and

Turkel/7/. The resulting block-bidiagonal matrices are straightforward inverted with the procedure similar to the implicit MacCormack method. These inversions are easy to program and vectorize.

B. The Navier-Stokes equations

The two-dimensional compressible Navier-Stokes equations are written in the conservation-law form,

$$U_t+F_x+G_y=Re^{-1}(R_x+S_y), \tag{16}$$

$$U=(\rho, \rho u, \rho v, e)^T,$$

$$F=(\rho u, \rho u^2+p, \rho uv, u(e+p))^T,$$

$$G=(\rho v, \rho uv, \rho v^2+p, v(e+p))^T,$$

$$R=(0, \tau_{xx}, \tau_{xy}, r)^T,$$

$$S=(0, \tau_{xy}, \tau_{yy}, s)^T,$$

$$\tau_{xx}=(\lambda+2\mu)u_x+\lambda v_y,\ \tau_{xy}=\mu(u_y+v_x),\ \tau_{yy}=(\lambda+2\mu)v_y+\lambda u_x,$$

$$r=u\tau_{xx}+v\tau_{xy}+\alpha(c^2)_x,\ s=u\tau_{xy}+v\tau_{yy}+\alpha(c^2)_y,$$

$$\alpha=\mu/Pr(\gamma-1).$$

The superscript T denotes transpose of a vector. A perfect and calorically perfect gas is assumed as follows.

$$p=(\gamma-1)(e-\rho(u^2+v^2)/2),\quad c^2=\gamma p/\rho . \tag{17}$$

The bulk viscosity for diatomic gas, $\lambda+2\mu/3$, can be taken neary equal to $2\mu/3$, and thus it is assumed that $\lambda=0$ /8/.

The Beam-Warming-Steger method/5,6/ applied to Eqs.(16) results in the following approximate factorization,

$$\begin{aligned}&(I+hD_i(A+P))(I+hD_j(B+Q))\Delta U_{ij}^{\,n}=-hLr_{ij}^{\,n},\\ &Lr_{ij}^{\,n}=D_i(F_{ij}^{\,n}-R_{ij}^{\,n}/Re)+D_j(G_{ij}^{\,n}-S_{ij}^{\,n}/Re),\\ &A=\left(\frac{\partial F}{\partial U}\right)_{ij}^{\,n},\quad B=\left(\frac{\partial G}{\partial U}\right)_{ij}^{\,n},\end{aligned} \tag{18}$$

where $U_{ij}^{\,n}=U(i\Delta x,\ j\Delta y,\ n\Delta t)$, D_i and D_j are the difference operator for i and j, respectively, and $h=\Delta t/\Delta x=\Delta t/\Delta y$. The viscous terms R and S are linearized as follows/6/. The elements of R are of the general form: $f_m=a_m\partial b_m/\partial x$. Each element linearizes in time;

$$\Delta f_m^{\,n}=a_m\frac{\partial}{\partial x}\left(\sum_{m'}\frac{\partial b_m}{\partial q_{m'}}\Delta q_{m'}^{\,n}\right), \tag{19}$$

where q_m indicates the element of U and it is assumed that $\partial a_m/\partial q_m=0$. This algorithm requires inversions of the block-tridiagonal matrices composed of the block matrices A, B, P and

Q.

The Jacobian matrices A and B are diagonalized/1/ as,

$$A=XE_AX^{-1},\ B=YE_BY^{-1}, \tag{20}$$

$$E_A=\mathbf{diag}(u,u,u+c,u-c) \text{ and } E_B=\mathbf{diag}(v,v,v+c,v-c),$$

where X and Y are the eigenvector matrices. The diagonal matrices E_A and E_B can be split along the sign of each eigenvalue;

$$E_A=E_A^{+}+E_A^{-} \text{ and } E_B=E_B^{+}+E_B^{-}. \tag{21}$$

The operators in Eq.(18) can be replaced by using the flux vector splitting/3/, for example,

$$D_iA=D_{i-}XE_A^{+}X^{-1}+D_{i+}XE_A^{-}X^{-1}. \tag{22}$$

The LU factored form can be obtained as,

$$I+hD_i(A+P)=(I+hD_{i-}(XE_A^{+}X^{-1}+\hat{P}))(I+hD_{i+}(XE_A^{-}X^{-1}-\hat{P})), \tag{23}$$

if D_iP can be rewritten as $D_{i-}\hat{P}-D_{i+}\hat{P}$. The eigenvalues of the block matrix $\hat{P}$ are related to the stability for the discretized viscous terms. On the other hand, smoothing terms can be added to the flux vector as a weight of upwind differences/3/;

$$\hat{E}_A^{\pm} = E_A^{\pm} + kI^{\pm}, \tag{24}$$

where $I^{\pm} = \mathbf{sign}(E_A^{\pm})$. The parameter k can be chosen so as to maintain the stability of the viscous terms as follows,

$$k=\frac{\nu}{Re\rho\Delta x},\ \nu=\mathbf{max}(2\mu,\lambda+2\mu,\frac{\gamma\mu}{Pr}). \tag{25}$$

This estimation is similar to the implicit MacCormack scheme. Furthermore, ν is identically set to 2μ if $\lambda=0$, $\gamma=1.4$ and $Pr=.7$.

Finally, the LU factored scheme is described as,

$$(I+hD_{i-}\hat{A}^{+})(I-hD_{i+}\hat{A}^{-})(I+hD_{j-}\hat{B}^{+})(I-hD_{j+}\hat{B}^{-})\Delta U_{ij}^{n}=-hLr_{ij}^{n},$$

$$\hat{A}^{\pm} = X|E_A^{\pm} + kI^{\pm}|X^{-1},\ \hat{B}^{\pm} = Y|E_B^{\pm} + kI^{\pm}|Y^{-1}, \tag{26}$$

$$k=\frac{2\mu}{Re\rho\Delta x}=\frac{2\mu}{Re\rho\Delta y},$$

where the absolute value of a matrix is defined as the matrix whose elements are replaced by their absolute values.

The usual fourth-order dissipation/5,6/ is added to the right-hand-side of Eq.(26). On the other hand, the implicit smoothing terms are not required in the following test problem.

The resulting scheme is of $O(\Delta t, \Delta x^2)$ and unconditionally stable for linearized analysis. It is efficient, and needs less temporary storage because no inversion of block-tridiagonal matrix is required. It is also easy to program and vectorize because the only implicit operators of the Beam-Warming-Steger

method should be rewritten and the resulting procedure is similar to the implicit MacCormack one.

§3. The Interaction Problem on a Flat Plate

The interaction problem of shock wave with laminar boundary layer on a flat plate/9-14/ was solved as a test for the present scheme. The typical feature is represented by the numerical pressure contour map in Fig.4d. An oblique shock wave is incident on a laminar boundary layer. The regular reflection imposes pressure gradients on the boundary-layer flow. When the adverse pressure gradient is sufficiently large, the boundary layer separates. The resulting streamline curvature generates reflected shock waves. At the leading edge, a curved bow shock wave appears due to the streamline curvature associated with formation of the boundary layer.

The computational mesh (Fig.1) at first contained 32x32 mesh-points. The mesh increments were uniform in the x direction as $\Delta x=1/15$ and exponentially stretched in the y direction as $\Delta y_j = \Delta y_{min} \times 1.17^j$ where $\Delta y_{min}=8.31\times10^{-4}$. Mesh-points successively increased by multiples of 32 to 256 points in the x direction and to 96 points in the y direction. The mesh increments decreased, corresponding to mesh refinement. The shock angle was set to 32.6 degrees, the freestream Mach number; 2.0, and the Reynolds number based on the distance from the leading edge to the shock impinging location; 0.296×10^6. Molecular viscosity was calculat-

ed by Sutherland's formula. The Prandtl number was set to .7 and assumed to be constant.

The initial condition was taken to be uniform flow. The computation was impulsively started. The incident shock wave was given at the top of the computational region as the fixed boundary conditions. The upstream boundary conditions were also fixed because the freestream was supersonic. The zero-order extrapolation was employed at the boundary of outflow. The reflective boundary conditions were used at the plane of symmetry and the wall; U_{1j}=**diag**(1,1,-1,1)U_{2j} and U_{1j}=**diag**(1,-1,-1,1)U_{2j}, respectively.

The implicit boundary condition of ΔU^n at outflow was taken equal to 0. In the y direction, the implicit procedure swept first from the top with ΔU^n=0 to the wall, then swept to the contrary. The boundary flux of the later sweep was set to 0.

The results for 32x32 and 64x32 mesh-points were obtained when the residual ΔU reached 10^{-3}, and those for 128x64 and 256x96 mesh-points, when 5×10^{-4}. The smoothing coefficient for the former was set to the usual value, Δt. That for the latter was taken equal to $3\Delta t$, since the actual stability lessened in the region of the reflected expansion wave on the boundary layer.

Figures 2a and 2b compare the surface pressure and the skin friction distributions calculated by the present scheme for 64x32 mesh-points with those by the experiment/13/. Figs.3a and 3b show those for 128x64 mesh-points. In the pressure distribution, the peak at the leading edge and the plateau at the separated

region are clearly observed. The numerical pressure contours for 32x32 to 256x96 mesh-points were presented in Figs.4a to 4d where the lines indicate the contours of values of 1.05 to 1.40 at intervals of .05. Shock waves appeared as a near discontinuity owing to mesh refinement, such as the bow shock wave and the double reflected shock waves. Fig.5 shows various numerical contour maps near the location of incidence for 256x96 mesh-points. In Fig.5c, incomressibilty was assumed to evaluate stream function which was set to 0 at the wall and multiplied by 10^2. The skin friction distribution in Fig.3b suggests a structure of the separated bubble, and this is consistent with that obtained in Fig.5c. These results are consistent with the experimental and other numerical results.

The CPU time per step is reduced about 20% compared with that of the implicit MacCormack method. The maximum CFL numbers were about 60 in the present computations. For the two finer meshes, the run times required to reach the steady state were about 15 in nondimensional time. The convergence rates in mesh refinement decreased owing to the time increments bounded by the actual stability.

§4. The Interaction Problem on an NACA0012 Airfoil

Algebraic grid generation technique is applied to iteratively construct the nearly orthogonal grid system around an NACA0012 airfoil. The lack of smoothness is overcome by averaging grid points. The concentration to the boundary layer is smeared out

near the trailing edge. Mesh refinement in the direction along the body and wake is carried out in order to capture the very fine vortex motion. The number of the used grid points is mainly 321x41 points.

The detailed flow field at the Mach number, .75, and the Reynolds number, 10^5, is shown in Fig.6 to 9. A lot of small separation bubbles are produced around the upper surface of the airfoil in a very short time. The boundary layer becomes thick suddenly. Then the bubbles flow away and the boundary layer returns to thin.

Fig.10 shows the numerical results in the inviscid case. Fig.11 shows the results in the turbulent case for 81x41 mesh-points by using an algebraic two-layer eddy viscosity model due to Baldwin and Lomax. Both results resemble each other.

For the lower Reynolds number, the separation becomes large and the shock wave disappears(Fig.12). On the other hand, the separation bubbles become very small and the almost steady shock wave is found for the higher Reynolds number(Fig.13 and 14).

Finally the Mach number is set to .95 (Fig.15). The shock wave moves to the trailing edge and the separation is suppressed. The lamda shock wave is also found at the upper surface of the airfoil.

Transonic flows with viscous-inviscid interactions have been successfully simulated by directly computing the compressible Navier-Stokes equations.

References

1) R. F. Warming, R. M. Beam and B. J. Hyett, Math. Comput. **29** (1975), 1037.

2) T. H. Pulliam and D. S. Chaussee, J. Comput. Phys. **39** (1981), 347.

3) J. L. Steger and R. F. Warming, J. Comput. Phys. **40** (1981), 263.

4) R. W. MacCormack, AIAA J. **20** (1982), 1275.

5) R. M. Beam and R. F. Warming, J. Comput. Phys. **22** (1976), 87.

6) J. L. Steger, AIAA J. **16** (1978), 679.

7) A. Jameson and E. Turkel, Math. Comput. **37** (1981), 385.

8) S. Chapman and T. G. Cowling, "The Mathematical Theory of Non-Uniform Gases," Cambridge Univ. Press, Cambridge, 1952.

9) R. W. MacCormack, Proc. 2nd I.C.N.M.F.D., Lecture Notes in Physics, vol.8 Springer-Verlag, Berlin Heidelberg New York, 1971.

10) R. W. MacCormack and B. S. Baldwin, AIAA paper 75-1.

11) R. M. Beam and R. F. Warming, AIAA J. **16** (1978), 393.

12) J. D. Murphy and L. S. King, AIAA paper 83-0134.

13) R. J. Hakkinen, I. Greber, L. Trilling and S. S. Abarbanel, NASA Memo 2-18-59W, 1959.

14) A. H. Shapiro, "The Dynamics and Thermodynamics of Compressible Fluid Flow," Volume I and II, John Wiley & Sons, New York, 1954.

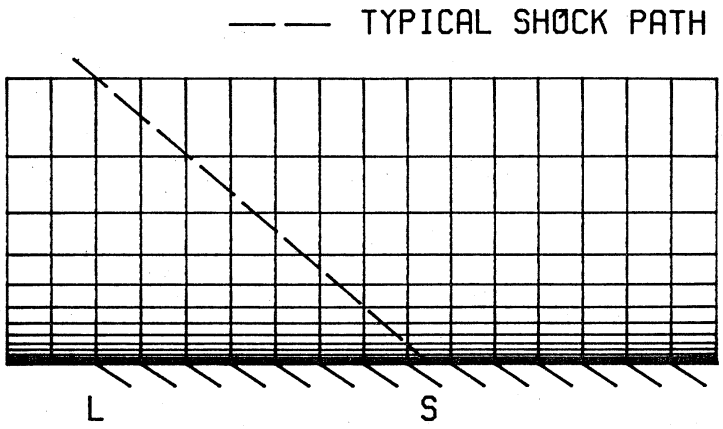

Fig.1 Computational mesh and incident shock wave.
Shock angle ϕ=32.6°, Mach number M=2.0, Reynolds' number Re=.296x10^6.
L; the leading edge, S; the incident point of shock wave.

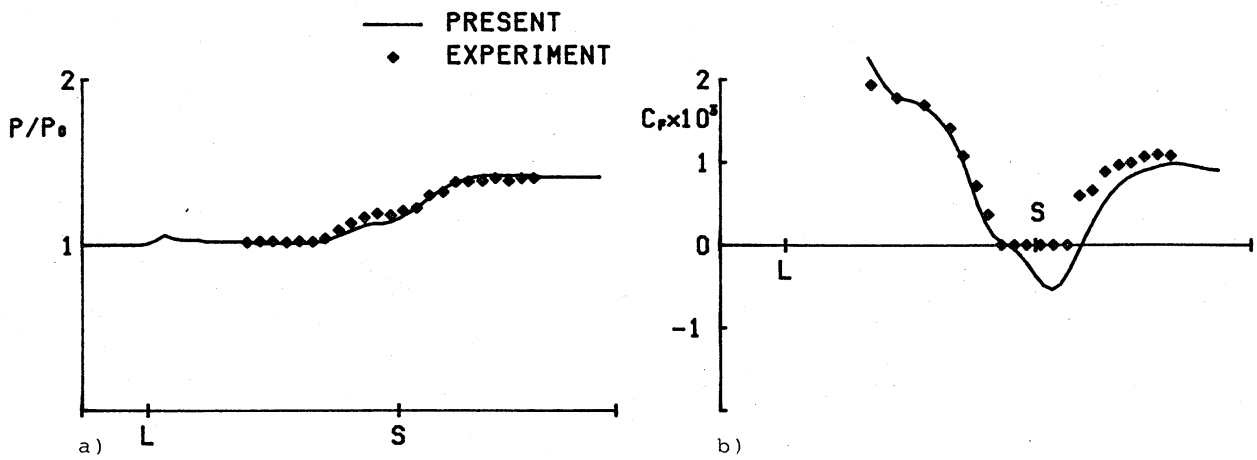

Fig.2 Numerical results for 64x32 mesh-points.
a) surface pressure, b) skin friction.

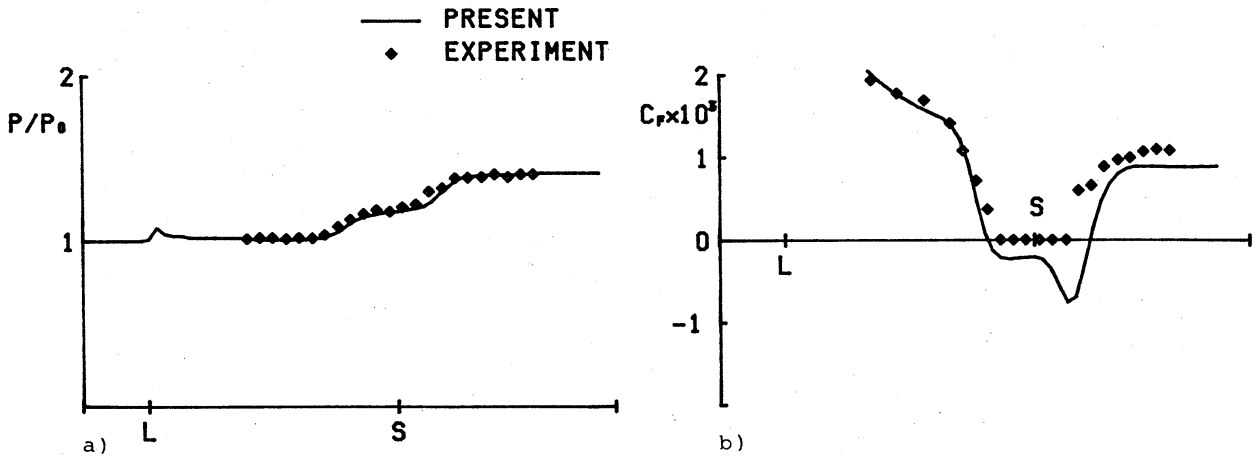

Fig.3 Numerical results for 128x64 mesh-points.
a) surface pressure, b) skin friction.

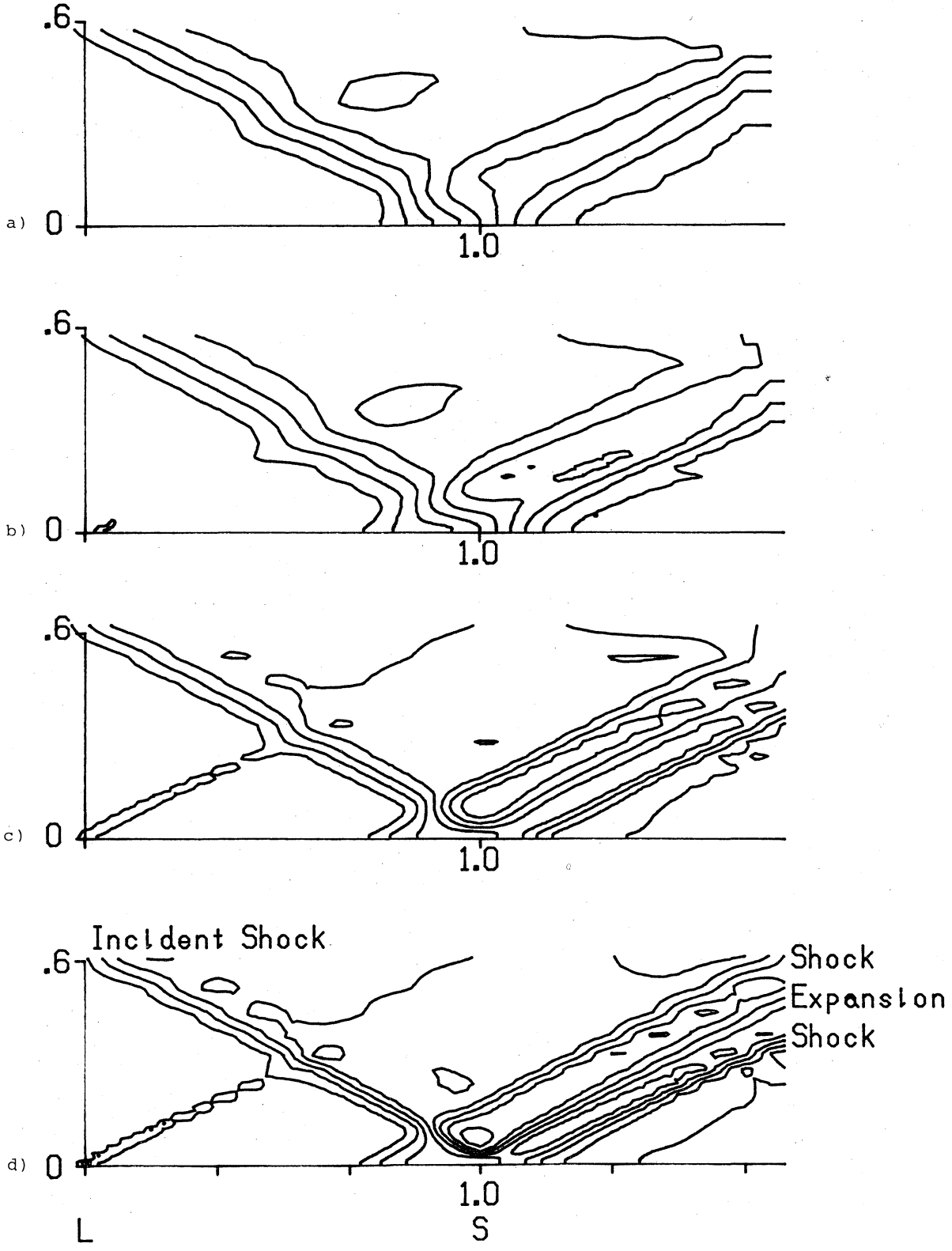

Fig.4 Numerical pressure contours.
a) 32x32 mesh-points, b) 64x32 mesh-points,
c) 128x64 mesh points, d) 256x96 mesh-points.

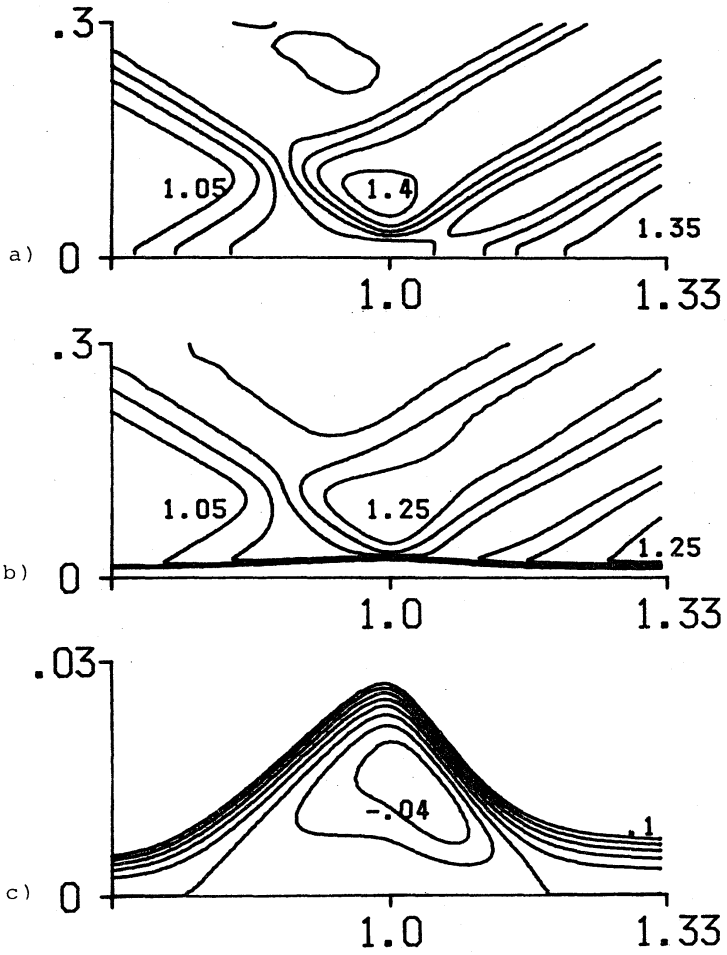

Fig.5 Numerical contour maps near the incident point of shock wave for 256x96 mesh-points.
a) pressure contours at intervals of .05, b) density contours at intervals of .05, c) stream function contours at intervals of .02.

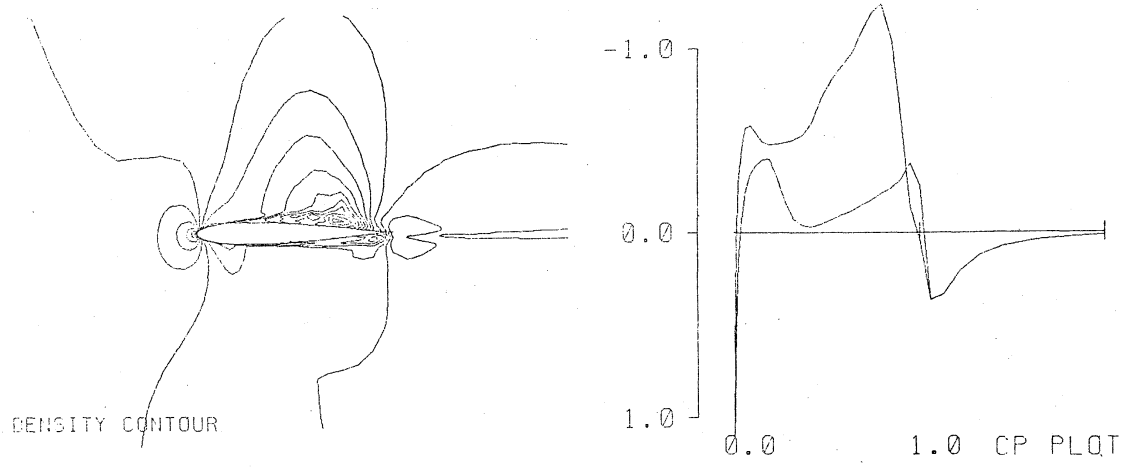

Fig.6 Numerical results for NACA0012 airfoil at an angle of attack of 2 degrees in case of M=.75, Re=10^5 and T=10.

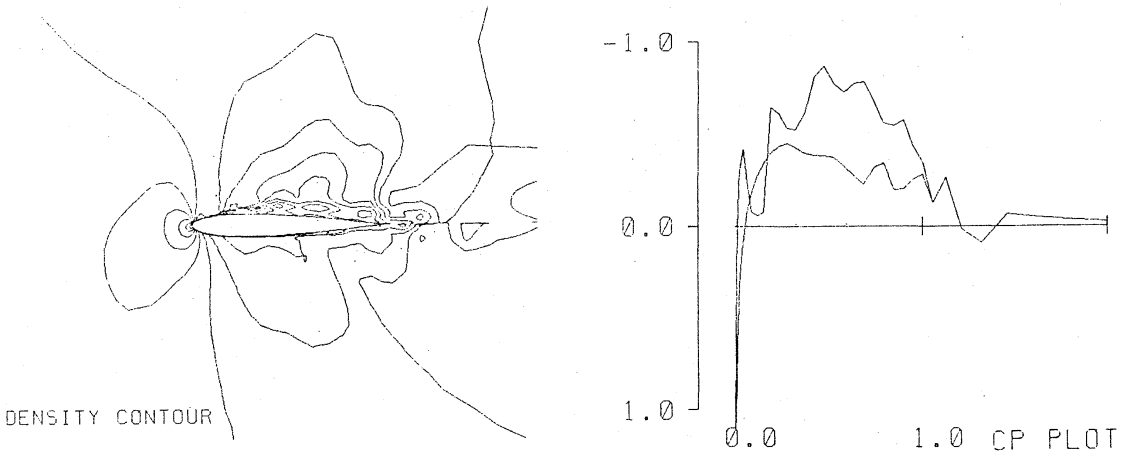

Fig.7 M=.75, Re=10^5, and T=17.

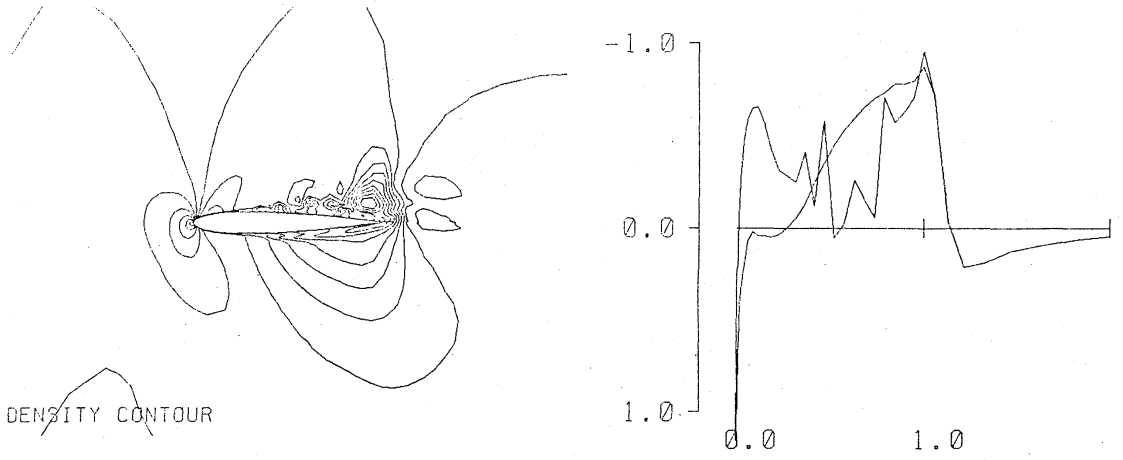

Fig.8 M=.75, Re=10^5, T=24.

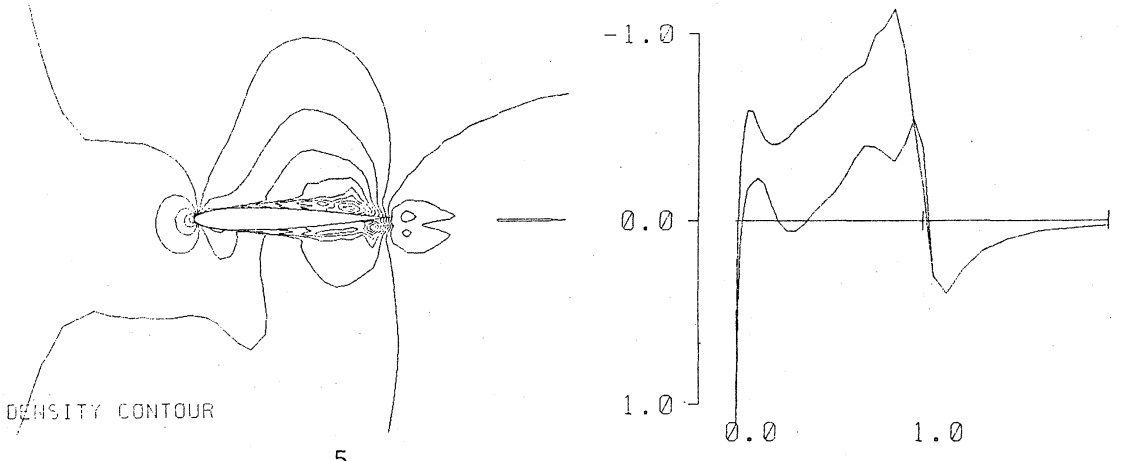

Fig.9 M=.75, Re=10^5, T=31.

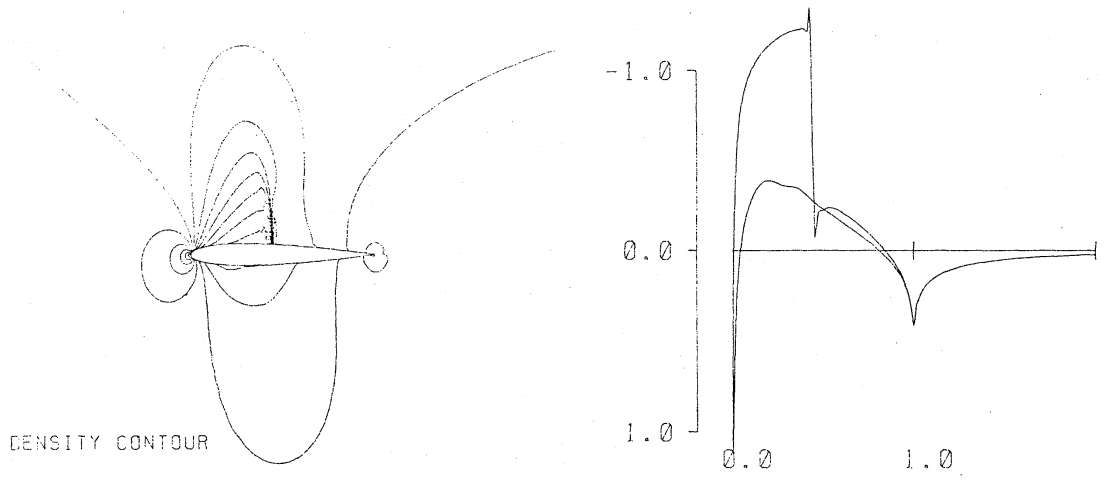

Fig.10 M=.75, inviscid flow.

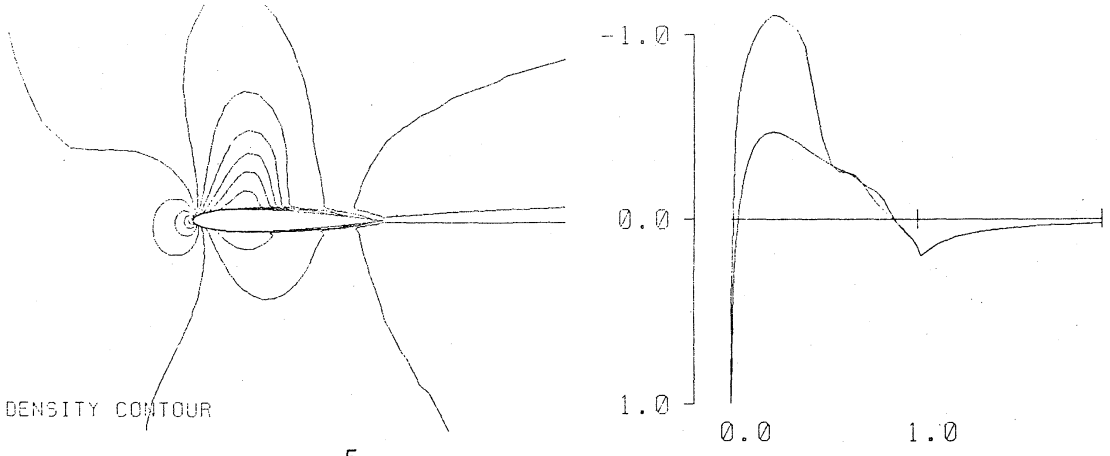

Fig.11 M=.75, Re=10^5, Baldwin-Lomax turbulence model, 81x41 mesh-points.

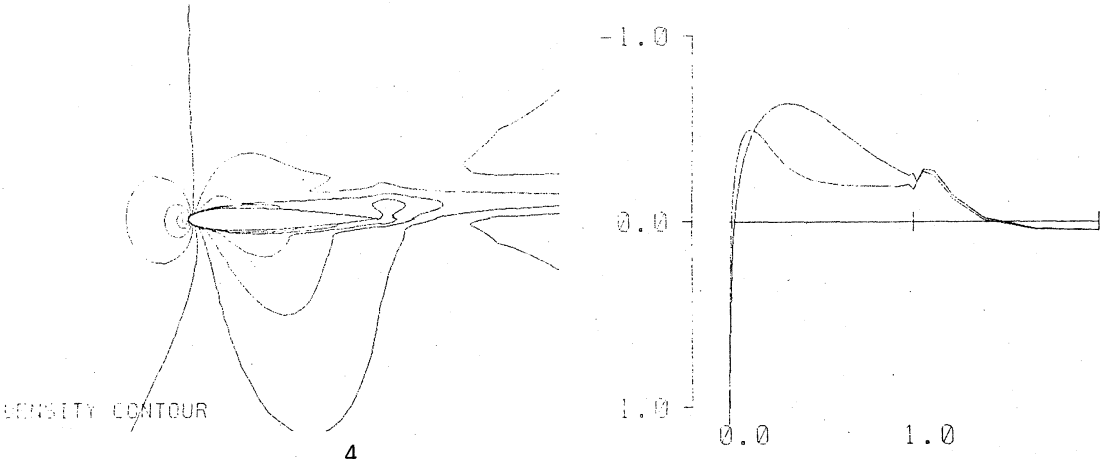

Fig.12 M=.75, Re=10^4, 81x41 mesh-points.

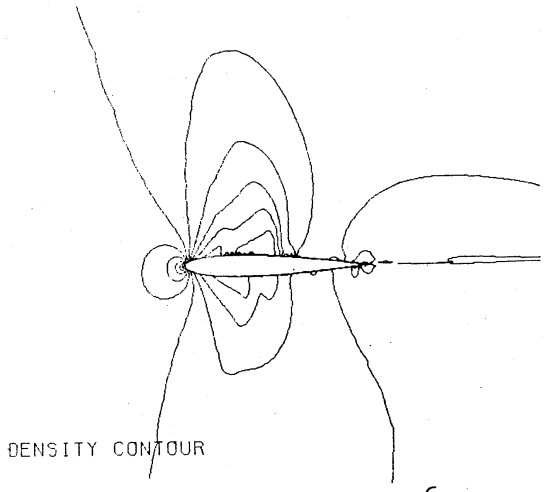

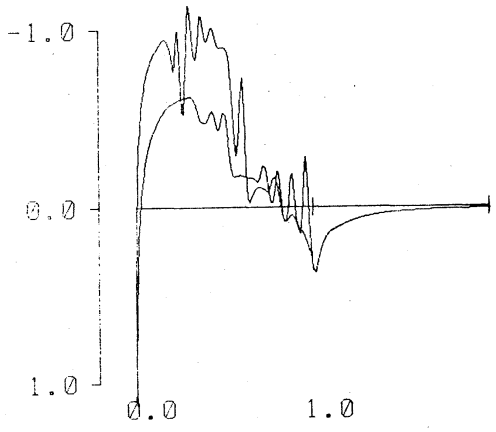

Fig.13 M=.75, Re=6.7x10^6, T=5.

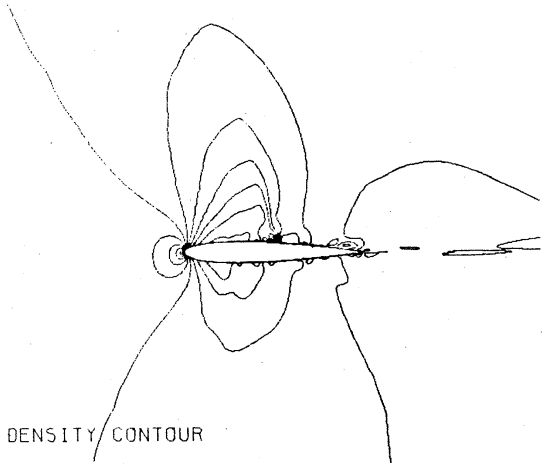

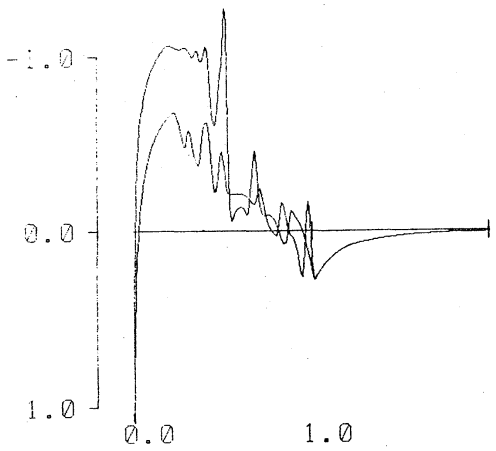

Fig.14 M=.75, Re=6.7x10^6, T=6.

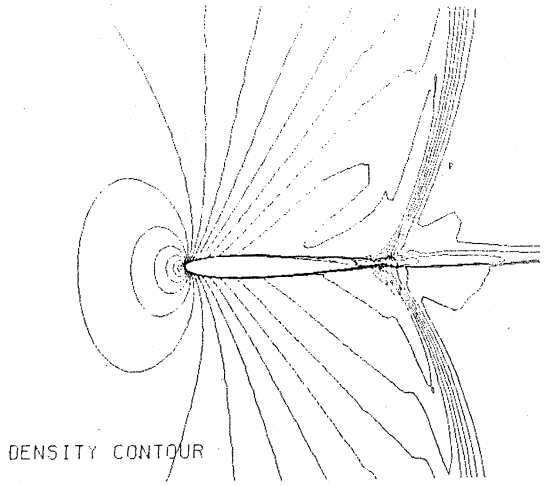

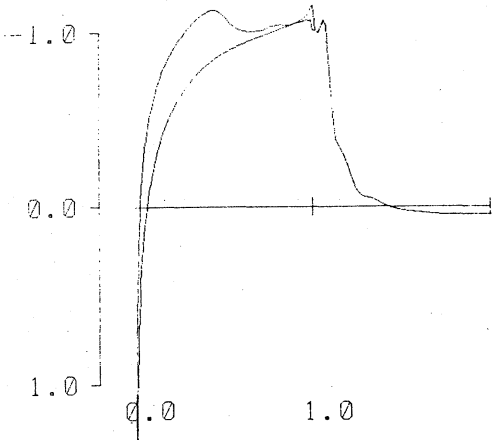

Fig.15 M=.95, Re=10^5.